Magnetic Field Generated by Double-Circuit Twisted Three-Phase Cable Lines

**Giovanni Mazzanti, Marco Landini*, Effrosyni Kandia,
Andrea Bernabei, and Marco Cavallina**

Abstract—The evaluation of the magnetic field from double-circuit twisted three-phase power cable lines misses a sound and exhaustive theoretical and experimental treatment in the literature. This paper presents a rigorous approach to the calculation of the magnetic field from double-circuit twisted three-phase cables, whereby the magnetic field generated by such cables is computed as the vector sum of the two individual fields generated by each twisted three-phase cable. This approach is validated by means of extensive measurements of the magnetic field from single- and double-circuit twisted three-phase power cables — provided by Italian utilities — identical to those installed in the field.

1. INTRODUCTION

The search for environmentally friendly electricity and the concerns for power system effects on human health also involve power distribution. Lately, designing renewable energy projects also means taking actions for the reduction of the magnetic field generated by the power lines that connect renewable energy sources to the grid. Twisting of phase conductors is an effective magnetic field reduction tool [1–3]. Twisted three-phase cables are often used in MV and LV distribution networks and are the standard solution for connecting wind-generators and photovoltaic plants to the grid.

Still, computing the magnetic field associated with proposed electrical installations remains essential to demonstrate compliance with ICNIRP reference values [4], as well as to ensure that the magnetic induction values lie within the limits imposed by national and international laws to locations where persons spend significant amounts of time [5], and for the computation of the safety distances at which a maximum limit value of the rms magnetic induction is reached [6].

In the literature, some complex theoretical studies deal with the rigorous calculation of the magnetic field from single-circuit twisted three-phase cables [7–12]. Pettersson and Schönborg [1, 13] have proposed a dramatic simplification of such cumbersome calculation and have tested their approximated approach reproducing a single-circuit twisted three-phase cable via three plastic coated $50\,\text{mm}^2$ stranded Cu-wires that were helically wound on a plastic pipe. In [14], a simplified formula that has advantages over that by Pettersson and Schönborg is proposed thereby completing the picture about single circuits.

Actually, electric utilities are interested also in double-circuit twisted three-phase cable lines, as well as in multiple-circuit (i.e., more than two) twisted three-phase cable lines, both in overhead and in underground layout [15]. Unfortunately, double- and multiple-circuit twisted cable lines fall among complex electromagnetic field configurations for which, as to our best knowledge, rigorous analytic calculation tools are missing in the literature to date; such tools would enable a fast and accurate evaluation of the magnetic field. An alternative would be the use of finite element methods (FEM), but such methods require the use of complex and costly computer codes that take a lot of computing

resources and time: a comparison with FEM is beyond the scope of this paper (although it is planned as a future development of this investigation). Furthermore, reliable measurement results of the magnetic field generated by double- and multiple-circuit twisted three-phase power cables are not available in the literature.

In fact, as to the calculation tools the authors of this paper have proposed for the first time an approach that is based on the "worst case assumption": the rms magnetic field B generated by a double-circuit twisted cable line is calculated as the algebraic sum of the two single-circuits fields [15]. It can be argued that this approach is the most conservative, but it is also strongly-approximated. As to the measurements, Karady et al. reported in [16, 17] results relevant to a double-circuit twisted three-phase cable: the cable consists of two identical 600 V triplex XLPE underground cables each made of two phase conductors plus one neutral conductor (of different cross-section and carrying opposite current), twisted together to produce the triplex cable configuration. It can be argued that this configuration is rather different from that of existing double-circuit twisted three-phase power cable lines.

This paper tries to fill both the theoretical and experimental gaps in the literature about double-circuit twisted three-phase power cable lines. Indeed, on the one hand a rigorous procedure for the calculation of the magnetic field from such lines is proposed, whereby the rigorous calculation of the magnetic field from each single-circuit twisted three-phase cable is performed first, and the vector sum of the magnetic fields from each cable is carried out later via the composition of the three- dimensional magnetic field components, so as to yield the total magnetic field generated by both circuits. On the other hand, this theoretical approach is validated via extensive measurements of the magnetic field generated by double-circuit three-phase twisted power cables provided and frequently used by Italian utilities. In this way, differently from [16, 17], all measurements are relevant to three phase conductors of the same size carrying the same rms current without the presence of a neutral conductor. Furthermore, these extensive double-circuit measurements concern two different types of twisted three-phase power cables used for power distribution at the MV level.

2. DOUBLE-CIRCUIT TWISTED CABLE LINES: THEORY

2.1. Exact Vector Sum

The exact theoretical study of the magnetic field from a double-circuit twisted three-phase cable line is based on some assumptions, namely: the twisted cables are indefinitely long; their axes are straight and parallel to each other; their currents are in-phase; the surrounding media is linear, thus the superposition principle applies. Then, the two individual magnetic fields generated by each circuit can be calculated separately at every field-point and composed linearly thereafter. This composition requires, firstly, the conversion from the cylindrical to the Cartesian coordinate system and, subsequently, the vector sum of the magnetic-field Cartesian components in a "reference plane" where the field points of interest lie. This plane commonly coincides with a line section taken as orthogonal to the ground, the latter assumed as flat. For overhead cable lines — where cables hang from one pole to another at variable distances from the ground in a catenary-like shape — this section is usually the mid-span section, where the conductors are closest to the ground and hence the field is highest at the ground level. For underground cable lines, where cables in general run parallel to each other and to the ground, this section can be a particular section close to sensitive receptors. Hence, for both overhead and underground double-circuit twisted three-phase cable lines the "reference plane" for the magnetic field calculation can be taken as a Cartesian x-y plane orthogonal to the helix axis of both twisted three-phase cables, that is the Cartesian z-axis (or the cylindrical z-axis): this plane matches the equation $z = 0$. Thus, in order to describe the "exact" vector sum of the Cartesian components of the magnetic field for double-circuit twisted three-phase cable lines, let us first consider a "reference arrangement" of the double-circuit line in the "reference plane", such that the two cables hang on opposite sides of the poles at the same height from the ground, being d the horizontal distance between the two cables: for the sake of clarity, let us call "cable number 1" the twisted cable located in the semi-space where $x < 0$, while "cable number 2" is that located in the semi-space where $x > 0$.

Figure 1 is a sketch of the "reference arrangement": the radial field component, B_r, and the azimuthal field component, B_φ, generated by circuit 1 (light gray arrows) and 2 (dark gray arrows) are drawn qualitatively at five equally spaced field-points along the x-axis. This arrangement implies that
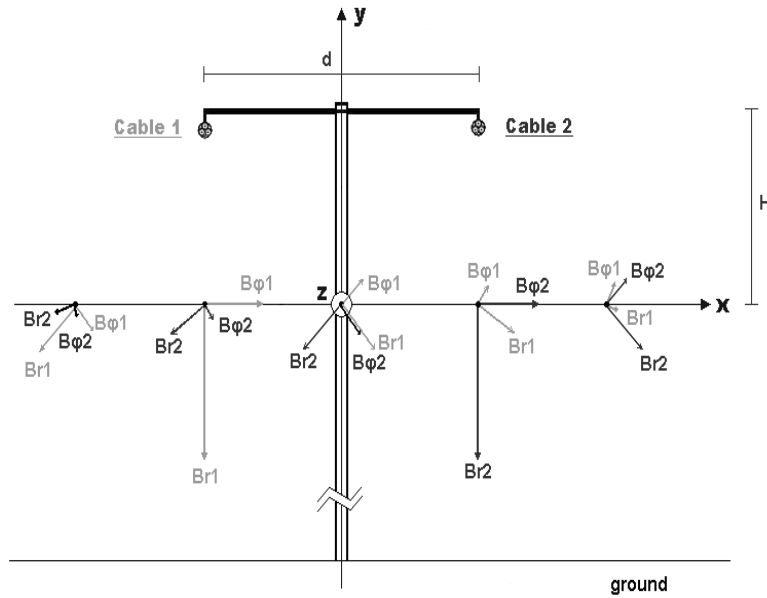
Figure 1. Sketch of the "reference arrangement" of the double-circuit twisted three-phase cable line chosen for the vector sum of the Cartesian components of the magnetic field. The relevant radial (B_r) and azimuthal (B_φ) field components generated by circuit 1 (light gray arrows) and 2 (dark gray arrows) at five equally spaced field-points along the x-axis are drawn qualitatively.

the radial component generated by either cable at a certain field point lies on the straight line connecting the cable axis with that point, while the azimuthal component from either cable is orthogonal to the radial component at every field-point. The axial component, B_z, at each field-point is omitted in Fig. 1 since the z-axis is orthogonal to the reference plane $z = 0$.

Based on Fig. 1, the magnetic field from the double-circuit, B_{DOUBLE}, can be computed as follows:

$$B_{DOUBLE} = \sqrt{B_x^2 + B_y^2 + B_z^2} \tag{1}$$

$$\begin{cases} B_x = B_{r1}\cos\theta_1 + B_{r2}\cos\theta_2 + B_{\phi1}\cos\varphi_1 + B_{\phi2}\cos\varphi_2 \\ B_y = B_{r1}\sin\theta_1 + B_{r2}\sin\theta_2 + B_{\phi1}\sin\varphi_1 + B_{\phi2}\sin\varphi_2 \\ B_z = B_{z1} + B_{z2} \end{cases} \tag{2}$$

where B_{r1}, B_{r2}, $B_{\varphi1}$, $B_{\varphi2}$ and B_{z1}, B_{z2} are the exact values of the radial, azimuthal and axial components of the magnetic field from circuit 1 and from circuit 2, respectively, and θ_1, θ_2, and φ_1, φ_2 are the angles formed by the x-axis and the radial, B_r, and azimuthal components, B_φ, from circuit 1 and 2, respectively (measured anticlockwise from the x-axis). B_{r1}, B_{r2}, $B_{\varphi1}$, $B_{\varphi2}$, B_{z1}, B_{z2} can be calculated via relationships in Eq. (6) after [1].

It holds:

$$\begin{cases} \theta_1 = \arctan(y_1/x_1) \\ \theta_2 = \arctan(y_2/x_2) \end{cases} \tag{3}$$

$$\begin{cases} \varphi_1 = \theta_1 + \pi/2 \\ \varphi_2 = \theta_2 + \pi/2 \end{cases} \tag{4}$$

(x_1, y_1) and (x_2, y_2) being, respectively, the coordinates of cables 1 and 2 in the plane $z = 0$, where φ reduces to Φ, the angle which indicates the angular position of the field-point in the twisted configuration [1, 13, 14].

The authors have implemented this theoretical approach in Matlab^{TM} environment, thereby attaining a code for calculating the magnetic field from double-circuit twisted three-phase cable lines. As a preliminary application of such code, let us focus into a practical problem involved by the vector

sum, i.e., the dependence of the components of the field of either cable (relationships in Eq. (6) after [1])) on Φ. Due to such dependence, performing the exact vector sum for the calculation of magnetic field at each x-y plane of interest requires knowing at that plane the angles Φ_1 and Φ_2 of the three phases of both twisted cables, i.e., the precise geometrical arrangement of the three phases of either cable. It can be argued that such phases arrangement can be hardly known in practice.

Aiming at checking the sensitivity of the magnetic field from the double-circuit, B_{DOUBLE} (see Eq. (1)), to the precise phases arrangement of either cable, let us consider what is referred to from now on as the "base case study", namely: the two twisted cable circuits displayed in Fig. 1 are ARG7H1RX [18] cables with cross-section $3 \times 120\,\text{mm}^2$, rated voltage 12(phase-to-ground)/20(phase-to-phase) kV, ampacity $I = 280\,\text{A}$, pitch $p = 1.37\,\text{m}$ and radius $\alpha = 0.020\,\text{m}$, placed at an horizontal distance $d = 1.0\,\text{m}$ from each other. A theoretically-infinite number of phases arrangement of either twisted cable is possible: let us choose here 16 different "base phases arrangements", of which 8 symmetric and 8 anti-symmetric, coupled together for the sake of convenience as shown in Table 1. As reported in the Table, each arrangement is characterized by its own dependence of Φ_1 and Φ_2 on θ_1 and θ_2, respectively. Hence (see Eq. (3)), for every arrangement Φ_1 and Φ_2 vary along the x-axis.

For each base phases arrangement, B_{DOUBLE} was computed by means of the above mentioned calculation code at five equally-spaced field points set along the x-axis from $x_{\min} = -1.0\,\text{m}$ to $x_{\max} = 1.0\,\text{m}$ at a vertical distance $H = 0.5\,\text{m}$ from cable axes. The values of B_{DOUBLE} of all 16 base phases arrangements in the five reference points are listed in Table 1, too, together with the relevant percent deviations $\Delta B\%$ from the values of B_{DOUBLE} obtained at the same five field-points by setting a constant value of $\Phi_1 = \Phi_2 = 60°$ — which yields the maximum value of magnetic field generated by each single circuit [14]. The main comments to these results are as follows:

1) For each of the 8 couples of symmetric and anti-symmetric base phases arrangements of Table 1, the ith symmetric arrangement i.a) provides the same values of the magnetic field at the same field-points as the ith antisymmetric arrangement i.b): this is the reason that the values of B_{DOUBLE} are reported only once for each couple;

2) The 16 base phase arrangements differ as to the values of Φ_1, Φ_2 at every field-point, but yield practically equivalent magnetic field profiles at the chosen line section;

3) For each of the 16 base phase arrangements, the values of B_{DOUBLE} obtained with the exact values of Φ_1, Φ_2 differ very slightly — always $< 1\%$ — from those obtained for $\Phi_1 = \Phi_2 = 60°$.

For this reason, the authors have chosen to set a constant value of $\Phi_1 = \Phi_2 = 60°$ at every field point in any case study. This choice corresponds to a phases arrangement that cannot be found in real double circuit twisted cable lines, but has two main advantages: it eliminates the need for the knowledge of the exact phases arrangement of either cable; it provides the maximum value of the magnetic field generated at every field point by each single circuit.
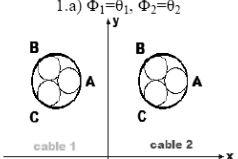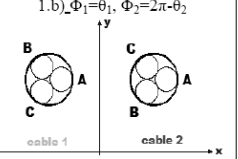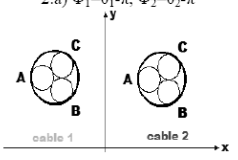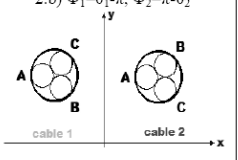
2.2. Algebraic Sum
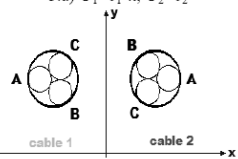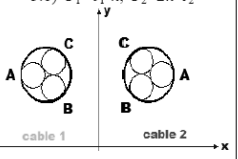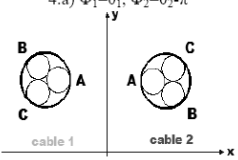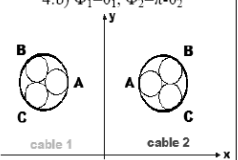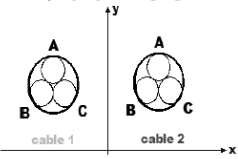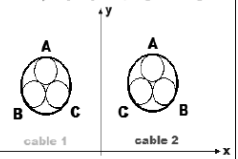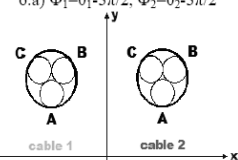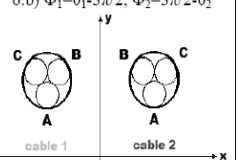
As pointed out in Section 1, an approximated method for the calculation of the magnetic field generated by a double-circuit twisted cable lines was proposed in [15]. This method, based on the same hypotheses outlined in Subsection 2.1 about the fie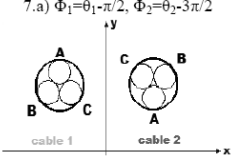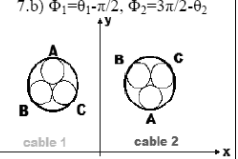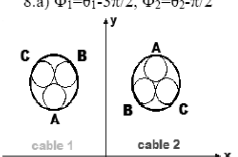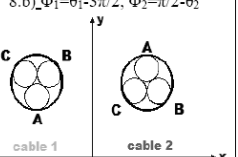ld, cable geometry, surrounding media and currents carried by the cables, relies on the so-called 'worst case' estimate. Namely, the magnetic field generated by the double-circuit twisted three-phase cable line, B_{WC}, is calculated as the algebraic sum of the two rms values of the field B generated by cable 1 and cable 2, B_1 and B_2 respectively, i.e.:

$$B_{WC} = B_1 + B_2 \tag{5}$$

This expression of B is drastically approximated, but it is also the most conservative one, hence it can serve as an upper limit reference for exposure evaluation purposes.

A comparison between the exact rms value of the total magnetic field B_{DOUBLE} according to Eq. (1) and the worst case estimate B_{WC} according to Eq. (5) for the base case study of Subsection 2.1 is displayed in Fig. 2, where the plots of B_{DOUBLE} and B_{WC} vs. horizontal distance x from the pole (i.e., from line axis) at a vertical distance $H = 0.5\,\text{m}$ from cable axes for $\Phi_1 = \Phi_2 = 60°$ are reported. As expected, the values of B_{WC} are larger than those of B_{DOUBLE} everywhere, but this is particularly evident at $x = 0$ — let us refer to such location as "equidistance axis of the cables" from now on — where B_{WC} overestimates B_{DOUBLE} up to $\sim 20\%$. The explanation for this is that the "worst case" estimate

Table 1. The 8 symmetric and the 8 anti-symmetric base phases arrangements of the "base case study", together with the corresponding values of B_{DOUBLE} after (1) calculated at five field-points as in Fig. 2 ($H = 0.5\,\mathrm{m}$, $X_{\min} = -1.0\,\mathrm{m}$, $X_{\max} = 1.0\,\mathrm{m}$) and the relevant percent deviations from the values of B_{DOUBLE} obtained for $\Phi_1 = \Phi_2 = 60°$ at the same field-points.

SYMMETRIC CASE-STUDIES	ANTI - SYMMETRIC CASE-STUDIES	B_{DOUBLE} [μT]	ΔB [%]
1.a) $\Phi_1=\theta_1$, $\Phi_2=\theta_2$	1.b) $\Phi_1=\theta_1$, $\Phi_2=2\pi-\theta_2$	$B_1=1.6986$ $B_2=5.7946$ $B_3=2.8197$ $B_4=5.8254$ $B_5=1.7010$	$\Delta B_1= -0.0910$ $\Delta B_2= -0.1774$ $\Delta B_3= 0.2194$ $\Delta B_4= -0.1505$ $\Delta B_5= -0.0153$
2.a) $\Phi_1=\theta_1-\pi$, $\Phi_2=\theta_2-\pi$	2.b) $\Phi_1=\theta_1-\pi$, $\Phi_2=\pi-\theta_2$	$B_1=1.6999$ $B_2=5.7946$ $B_3=2.8149$ $B_4=5.8254$ $B_5=1.6998$	$\Delta B_1= -0.0156$ $\Delta B_2= -0.1770$ $\Delta B_3= 0.0470$ $\Delta B_4= -0.1504$ $\Delta B_5= -0.0889$
3.a) $\Phi_1=\theta_1-\pi$, $\Phi_2=\theta_2$	3.b) $\Phi_1=\theta_1-\pi$, $\Phi_2=2\pi-\theta_2$	$B_1=1.6999$ $B_2=5.7946$ $B_3=2.8200$ $B_4=5.8254$ $B_5=1.7010$	$\Delta B_1= -0.0156$ $\Delta B_2= -0.1774$ $\Delta B_3= 0.2282$ $\Delta B_4= -0.1504$ $\Delta B_5= -0.0152$
4.a) $\Phi_1=\theta_1$, $\Phi_2=\theta_2-\pi$	4.b) $\Phi_1=\theta_1$, $\Phi_2=\pi-\theta_2$	$B_1=1.6986$ $B_2=5.7946$ $B_3=2.8147$ $B_4=5.8254$ $B_5=1.6998$	$\Delta B_1= -0.0910$ $\Delta B_2= -0.1770$ $\Delta B_3= 0.0392$ $\Delta B_4= -0.1505$ $\Delta B_5= -0.0889$
5.a) $\Phi_1=\theta_1-\pi/2$, $\Phi_2=\theta_2-\pi/2$	5.b) $\Phi_1=\theta_1-\pi/2$, $\Phi_2=\pi/2-\theta_2$	$B_1=1.6986$ $B_2=5.7946$ $B_3=2.8197$ $B_4=5.8254$ $B_5=1.7010$	$\Delta B_1= -0.0910$ $\Delta B_2= -0.1770$ $\Delta B_3= 0.0392$ $\Delta B_4= -0.1505$ $\Delta B_5= -0.0889$
6.a) $\Phi_1=\theta_1-3\pi/2$, $\Phi_2=\theta_2-3\pi/2$	6.b) $\Phi_1=\theta_1-3\pi/2$, $\Phi_2=3\pi/2-\theta_2$	$B_1=1.6999$ $B_2=5.7946$ $B_3=2.8149$ $B_4=5.8254$ $B_5=1.6998$	$\Delta B_1= -0.0156$ $\Delta B_2= -0.3575$ $\Delta B_3= 0.0392$ $\Delta B_4= -0.3012$ $\Delta B_5=-0.0152$
7.a) $\Phi_1=\theta_1-\pi/2$, $\Phi_2=\theta_2-3\pi/2$	7.b) $\Phi_1=\theta_1-\pi/2$, $\Phi_2=3\pi/2-\theta_2$	$B_1=1.6999$ $B_2=5.7946$ $B_3=2.8200$ $B_4=5.8254$ $B_5=1.7010$	$\Delta B_1= -0.0910$ $\Delta B_2= 0.0000$ $\Delta B_3= 0.0470$ $\Delta B_4= -0.3016$ $\Delta B_5= -0.0153$
8.a) $\Phi_1=\theta_1-3\pi/2$, $\Phi_2=\theta_2-\pi/2$	8.b) $\Phi_1=\theta_1-3\pi/2$, $\Phi_2=\pi/2-\theta_2$	$B_1=1.6986$ $B_2=5.7946$ $B_3=2.8147$ $B_4=5.8254$ $B_5=1.6998$	$\Delta B_1= -0.0156$ $\Delta B_2= -0.3552$ $\Delta B_3=0.2194$ $\Delta B_4= -0.0000$ $\Delta B_5=-0.0889$
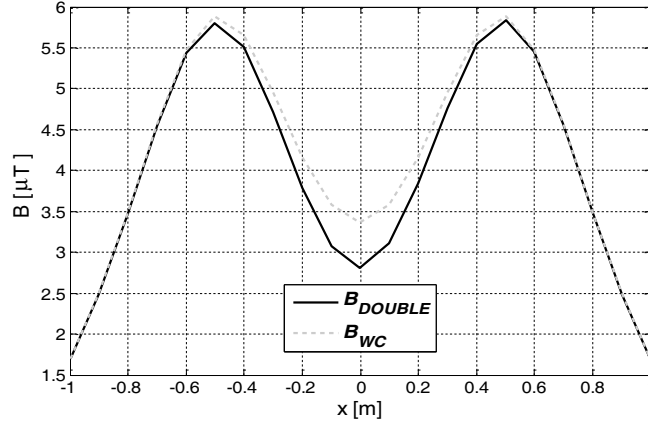
Figure 2. B_{DOUBLE} and B_{WC} vs. horizontal distance x for the base case study.
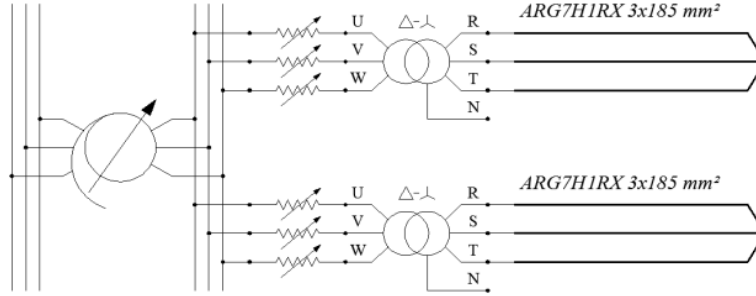
Figure 3. Sketch of the supply circuit in the experimental setup for the double-circuit twisted three-phase cable line.

results in an addition of the rms values of the magnetic field of the single-circuits in this area, whereas the exact vector analysis results in a subtraction of the magnetic field vectors of the single-circuits in the same area. Therefore, it is logical to obtain greater values with the "worst case" calculus.

3. DOUBLE-CIRCUIT TWISTED CABLE LINES: EXPERIMENTAL VALIDATION

3.1. Experimental Setup for the Double Circuit

The authors performed an extensive campaign of magnetic field measurements on double circuit twisted cables in order to validate the theoretical approach for the exact calculation of magnetic induction generated by double-circuit twisted cable lines (proposed in Subsection 2.1), and compare it with the worst-case approach illustrated in Subsection 2.1.

Figures 3 and 4 illustrate the experimental setup for the double-circuit twisted three-phase cables. Fig. 3 is a sketch of the supply circuit, consisting of a variac, six rheostats and two three-phase transformers and feeding the two twisted three-phase cables with balanced 40 A rms, 50 Hz phase currents. The two twisted cables chosen for the measurements were ARG7H1RX [18] cables with rated voltage 12(phase-to-ground)/20(phase-to-phase) kV, conductor cross-section $3 \times 185 \, \text{mm}^2$ and helix radius $\alpha = 0.022 \, \text{m}$. Fig. 4 is a view of the experimental setup, whereby one can see that the two cables were laid on the ground, at an horizontal distance $d = 0.50 \, \text{m}$ from each other, so as to preserve the parallelism of the two helixes and to keep their helix pitch p constant and equal to 1.4 m. Hence, the total length of either cable, $\approx 13 \, \text{m}$, is acceptable for simulating the infinite length case. For the sake of convenience, a Cartesian coordinate system similar to that of Fig. 1 was assumed, with the z-axis laying along the cable axes, the x-axis orthogonal to the cable axes and laying on the ground, and the y-axis orthogonal to the ground (see Fig. 4).
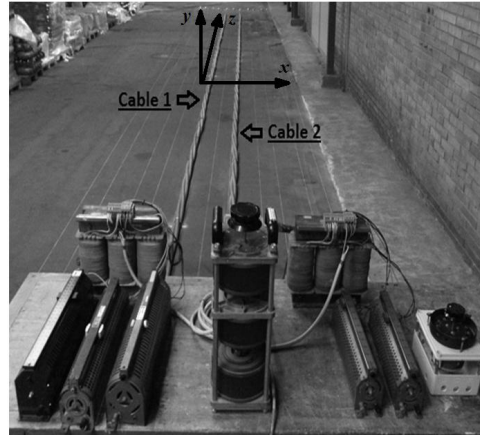
Figure 4. View of the experimental setup for the double-circuit twisted three-phase cable line (with cable numbers and Cartesian axes).

The magnetic field was measured using the Maschek ESM-100 meter, which features a concentric 5.6 cm-diameter spherical three-coil probe. The ground was divided into several corridors numbered according to the distances where the measurements took place along the x-axis. For each x distance, the field was measured at ten locations spaced 1.4 m along the cable axis — i.e., at ten contiguous multiples of the helix pitch from 0 to 9 — for z values from 0 m to 12.6 m, and the measurements at the mid cable length (say, $z = 5.6$ m) were used for comparison with the prediction of the numerical method in order to avoid any possible side effects. The measurements were repeated along the y-axis at 0, 0.3, 0.5, 0.8, 1.0 m height above each cable and above the equidistance axis of cables.

Afterwards, a complementary set of magnetic field measurements was taken, using the same three-coil magnetic-field meter and keeping the same experimental setup as in Figs. 3, 4 with the only difference that cable 2, as defined in Fig. 4, was replaced by an ARG7H1RX [18] cable with rated voltage 12(phase-to-ground)/20(phase-to-phase) kV, conductor cross-section $3 \times 120 \, \text{mm}^2$ and helix radius $\alpha = 0.020 \, \text{m}$.

It must be pointed out that preliminary measurements of the magnetic field in the experiment area in the absence of the cables were conducted, and the results showed a more than acceptable background magnetic induction of $\approx 40 \, \text{nT}$.

3.2. Measurements vs. Calculations

The input data of the code developed by the authors for computing the magnetic field from double-circuit three-phase twisted cables include: the rms phase currents, the pitch and radius of the helixes, and the x, y, z coordinates of the axes of both cables; the x, y, z coordinates of the field measuring point (center of the spherical coil sensor). Referring to the coordinate system of Fig. 4, the cables are located on the z-axis from $z = 0$ m to $z = 12.6$ m, considering as "cable 1" the twisted cable located in $x = -0.25$ and as "cable 2" that located in $x = 0.25$. The measuring points lie along the x-axis at different heights from the ground.

The code calculates the magnetic field components generated by either cable as a function of the radial distance r between the measuring point and the cable axis (Eqs. (6) from [11]), then it performs their exact vector sum (Eqs. (1)–(4)), along with their algebraic sum (Eq. (5)), and eventually yields a 2D plot of the corresponding profiles of total magnetic field, i.e., B_{DOUBLE} and B_{WC}, along the x-axis. By superimposing the measured field values, B_{meas}, to the above mentioned plots, Figs. 5–9 were derived concerning the double-circuit line with identical three-phase twisted cables (two ARG7H1RX $3 \times 185 \, \text{mm}^2$ cables with $p = 1.40$ m, $\alpha = 0.022$ m, $I = 40$ A) and Figs. 10–14 concerning the double-circuit line with three-phase twisted cables having different conductor cross-section (same cables, one with $3 \times 185 \, \text{mm}^2$ conductors, the other with $3 \times 120 \, \text{mm}^2$ conductors).

As shown in Figs. 5–14, generally speaking the agreement between the magnetic induction field calculated according to the exact vector sum, B_{DOUBLE}, and the measured values, B_{meas}, is satisfactory.
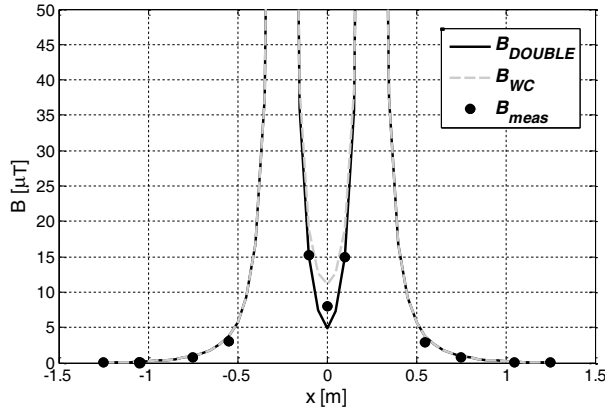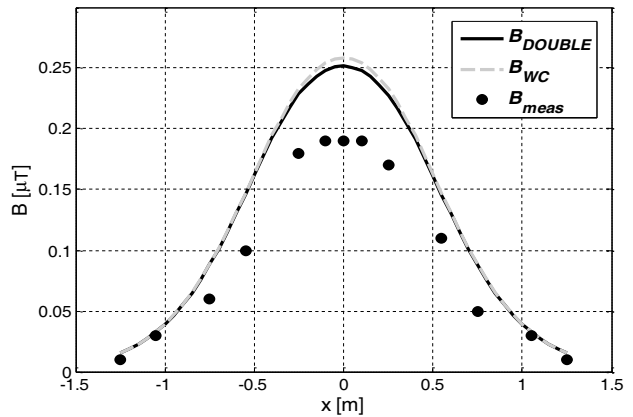
Figure 5. B_{DOUBLE}, B_{WC} and B_{meas} vs. x for double-circuit twisted three-phase cable lines with identical cables (ARG7H1RX 12/20 kV, $3 \times 185\,\text{mm}^2$, $p = 1.40\,\text{m}$, $\alpha = 0.022\,\text{m}$, $I = 40\,\text{A}$) at ground level ($y = 0\,\text{m}$) and mid cable ($z = 5.60\,\text{m}$).
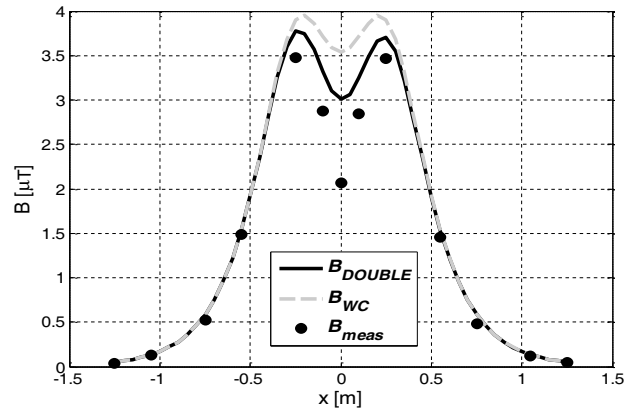
Figure 6. Same as Fig. 5, but at $0.3\,\text{m}$ from the ground ($y = 0.3\,\text{m}$).
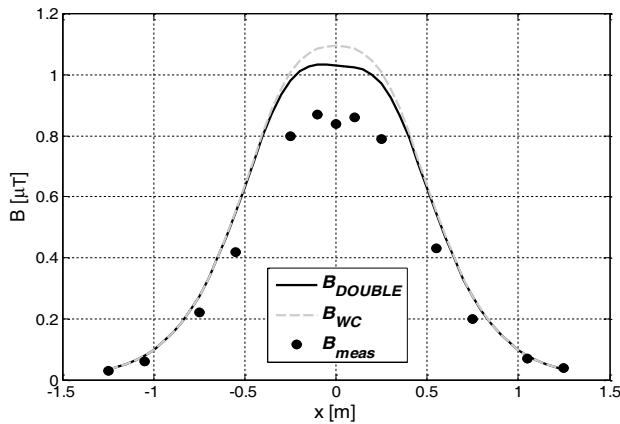
Figure 7. Same as Fig. 5, but at $0.5\,\text{m}$ from the ground ($y = 0.5\,\text{m}$).

Figure 8. Same as Fig. 5, but at $0.8\,\text{m}$ from the ground ($y = 0.8\,\text{m}$).

The overall relative percent error is within 20% maximum, except for some random singularities. These singularities can be explained as follows.

As previously hinted at, the experimental layout was arranged in such a way as to maintain the constancy of the pitch of the single helix along with the constancy of the perfect parallelism of the two helixes as much as possible, even by applying a mechanical tension to the cables by properly attaching them at their ends. However, some deviations from the constancy of the pitch and of the parallelism were unavoidable. Indeed, the cables were taken from coils wound and piled up for some time in the facilities of the utilities that have supplied them, hence — due to their own stiffness — they acquired and kept some shaping and irregularities of the pitch and of the parallelism. Such deviations are known to cause severe deviations of the field generated by double circuit twisted three phase cable lines from the theoretical field generated by such lines in the nominal "parallel and constant pitch configuration". Moreover, the exact location of the measuring probe affects the measurement value by much, since the magnetic field from twisted three phase cables changes dramatically with the distance of the field point from the cable axis. The experience gained during the experiment showed that deviations from the constancy of pitch and parallelism, on the one hand, and minor errors about the exact location of the measuring probe, on the other hand, have a dramatic impact on the deviation between measured
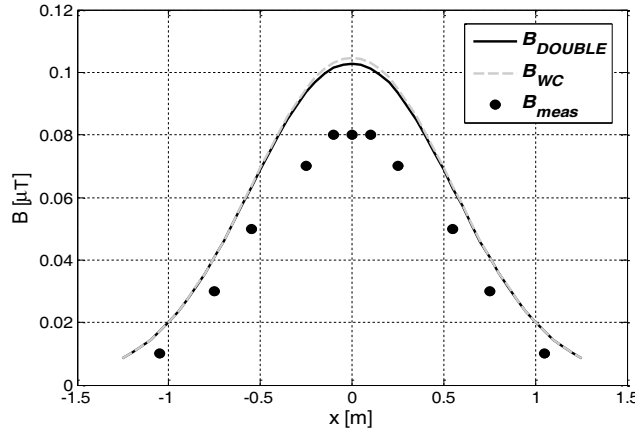
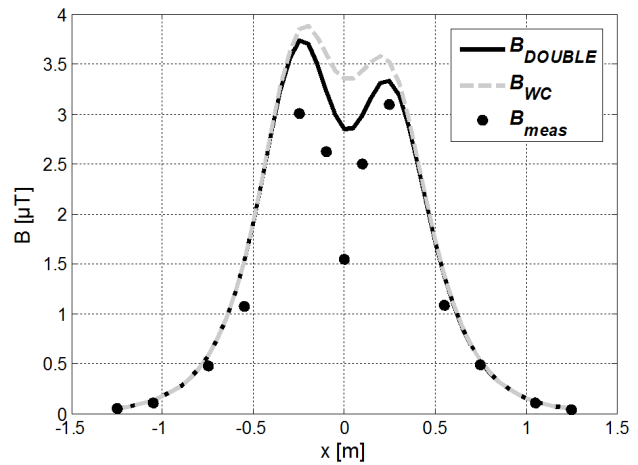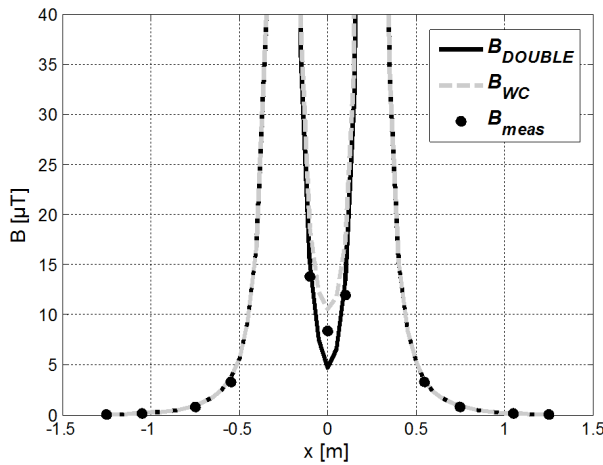**Figure 9.** Same as Fig. 5, but at 1.0 m from the ground ($y = 1.0$ m).

Figure 10. B_{DOUBLE}, B_{WC} and B_{meas} vs. x for double-circuit twisted three-phase cable lines with different cables (ARG7H1RX 12/20 kV, 3 × 185 mm^2, $p = 1.40$ m, $\alpha = 0.022$ m, $I = 40$ A and ARG7H1RX 12/20 kV, 3 × 120 mm^2, $p = 1.40$ m, $\alpha = 0.020$ m, $I = 40$ A) at ground level ($y = 0$ m) and mid cable ($z = 5.60$ m).

Figure 11. Same as Fig. 10, but at 0.3 m from the ground ($y = 0.3$ m).

and calculated values of the field. It is very difficult to avoid such deviations everywhere, and this is responsible for the major deviations observed in Figs. 5–14.

As anticipated in Subsection 2.2, the profiles of B_{WC} exhibit a maximum error in correspondence of the equidistance axis of the cables, that reduces as the distance of the field points from the equidistance axis increases. For distances > 0.5 m the B_{DOUBLE} and B_{WC} profiles are practically overlapped, although the error of B_{WC} remains always higher than that of B_{DOUBLE}.

Coming to the differences between Figs. 5–9 (identical cables) and Figs. 10–14 (different cables), in the latter the magnetic field values are higher close to the cable with larger conductor cross-section — thus larger helix radius α — although the helix pitch and rms currents are the same as in the former. Figs. 10–14 show in general a better agreement between calculated and measured field values for field points at distances from the ground in the range 0.5–1.0 m: the reasons for such better agreement need to be more deeply investigated.

As a general comment holding for both Figs. 5–9 and Figs. 10–14, B_{DOUBLE} seems to overestimate

the field in particular in the equidistance axis area. B_{WC} is a much simpler alternative to the exact calculus and behaves similarly to B_{DOUBLE} — although it features higher error, especially in the equidistance axis area. Thus B_{WC} can be a "quick-and-easy" calculation tool that provides magnetic field results close to the actual ones where the magnetic field is large enough for being detected by measurement instruments.

## 4. SINGLE-CIRCUIT TWISTED CABLE LINES: EXPERIMENTAL VALIDATION

Aiming at a broader assessment of the performances of the experimental setup and of the calculation code, the authors also performed measurements of the magnetic field generated by a single-circuit twisted three-phase cable line and compared them with the results provided by the calculation code.
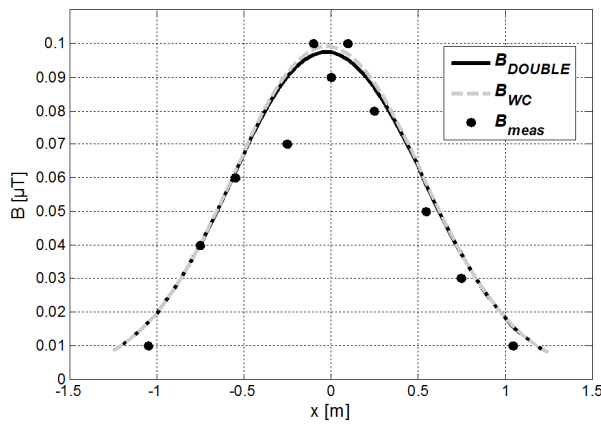
4.1. Experimental Setup for the Single Circuit

The measurements of the magnetic field generated by a single-circuit twisted three-phase cable line were conducted on the twisted three-phase cable ARG7H1RX with cross-section $3 \times 185\,\text{mm}^2$ ($\alpha = 0.022\,\text{m}$),
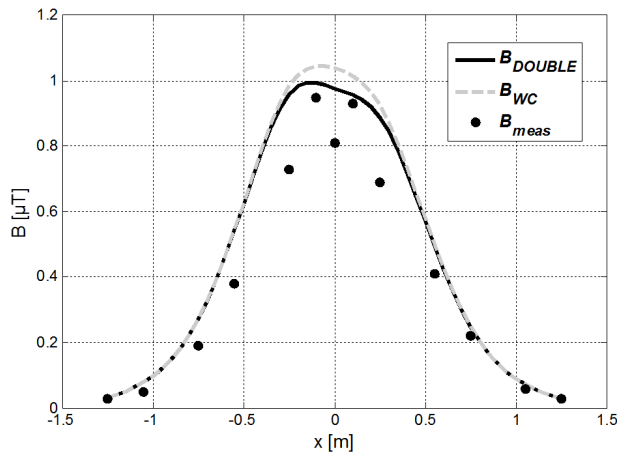
Figure 12. Same as Fig. 10, but at 0.5 m from the ground ($y = 0.5\,\text{m}$).
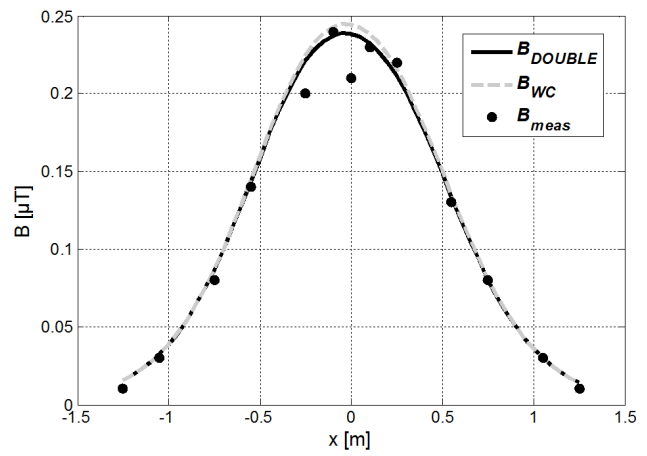
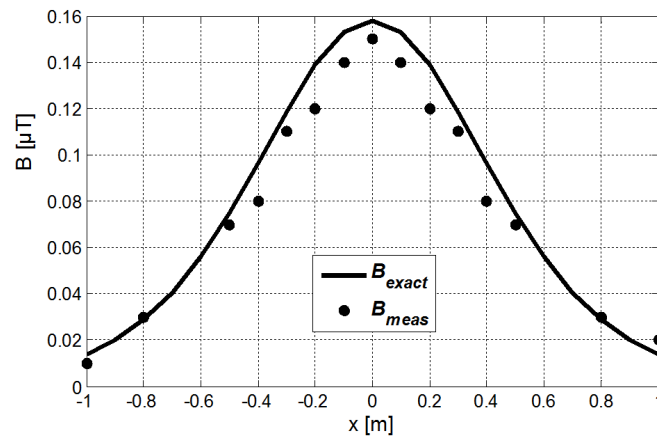**Figure 13.** Same as Fig. 10, but at 0.8 m from the ground ($y = 0.8\,\text{m}$).

Figure 14. Same as Fig. 10, but at 1.0 m from the ground ($y = 1.0\,\text{m}$).
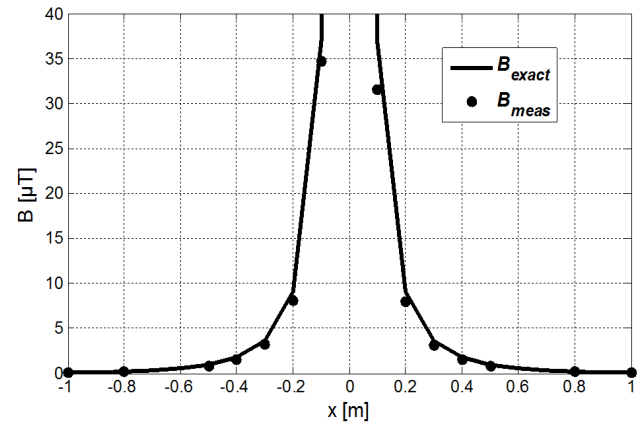
Figure 15. B_{exact} and B_{meas} vs. x for the cable ARG7H1RX 12/20 kV, $3 \times 185\,\text{mm}^2$ ($p = 1.40\,\text{m}$, $\alpha = 0.022\,\text{m}$, $I = 40\,\text{A}$) at ground level ($y = 0\,\text{m}$) and mid cable ($z = 5.60\,\text{m}$).

placed on the ground in the same way as in Fig. 4 so as to obtain a constant $p = 1.4$ m. The supply circuit, consisting now of a Variac, three rheostats and a three-phase transformer, fed the twisted three-phase cable with balanced 40 A, 50 Hz rms phase currents. As illustrated in Section 3.2, the measurements were performed at ten different locations spaced 1.4 m along the cable axis, and the measurements at the mid cable ($z = 5.60$) were compared with the predictions of the calculation code. At each location, two sets of measurements were carried out, one at ground level ($y = 0$) and another at a distance $y = 0.8$ from the ground, with the measuring points lying along the x-axis at various distances from the cable axis. The magnetic field was measured using again the magnetic-field meter Maschek ESM-100.

As shown in Figs. 15 and 16, the agreement between the measured field, B_{meas}, and the field calculated according to Eq. (7) from [1], B_{exact}, seems quite good for the examined distances from the cable axis, thereby proving the good performances of the experimental setup and of the calculation code also for a single-circuit twisted three-phase cable line.

Figure 16. Same as Fig. 15, but at 0.8 m from the ground ($y = 0.8$ m).

5. CONCLUSION

This paper has presented an exhaustive and sound theoretical treatment of the magnetic field emitted by an overhead or underground (the approach is the same) double-circuit twisted three-phase cable line, which includes the exact sum of the vector components for calculating the total field. The exact vector sum requires the computational hypothesis that the double-circuit twisted three-phase cable line is infinitely long with constant helix pitch of either cable and perfect parallelism of the two helixes. However, this is an ideal case that is never encountered in the practice. This involves unavoidable and non-negligible deviations between calculations and measurements, also because the latter are dramatically affected by the uncertainties in the exact location of the meter probe, especially in the case of twisted three-phase cables. Nevertheless, the agreement between the exact vector sum theory and the extensive measurements carried out by the authors is satisfactory, despite the above-mentioned difficulties in reproducing the ideal double-circuit twisted line in a test setup and in knowing its geometrical arrangement exactly. Moreover, the algebraic sum of the vector components for calculating the total field from the double circuit line (worst case approach) results a viable alternative to the exact vector sum, because of the simplicity of the former compared to the latter — at the expense of a moderately-higher error. This makes the calculation of the magnetic field generated by any multiple-circuit twisted three-phase power cable line — standard lines for transporting renewable energy — possible in the framework of a worst-case approach. Future work includes an in-depth analysis of the exact vector approach for multiple-circuit twisted three-phase cable lines, along with the appropriate experimental verification.

REFERENCES

1. Pettersson, P. and N. Schönborg, "Reduction of power system magnetic field by configuration twist," *IEEE Trans. on Power Delivery*, Vol. 12, No. 4, 1678–1683, Oct. 1997.

2. Lindberg, L., "Reduction of magnetic fields from electric power and installation lines," *IEE Proceedings — Science, Measurement and Technology*, Vol. 145, No. 5, 215–221, Sep. 1998.

3. Yang, C.-F., G. G. Lai, C.-T. Su, and H. M. Huang, "Mitigation of magnetic field using three-phase four-wire twisted cables," *Int'l Trans. on Electr. Energy Sys.*, Vol. 23, No. 1, 13–23, Jan. 2013.

4. International Commission for Non-Ionizing Radiation Protection (ICNIRP): "Guidelines for limiting exposure to time varying electric, magnetic and electromagnetic fields (up to 300 GHz)," *Health Physics*, Vol. 74, 494–522, Apr. 1998.

5. Council of the European Community (CEC): "Council Recommendation of 12 July 1999 on the Limitation of Exposure of the General Public to Electromagnetic Fields (0 Hz to 300 GHz)," *Official Journal of the European Communities*, L199, 59–65, 1999.

6. DPCM July 8th 2003, "Fissazione dei limiti di esposizione, dei valori di attenzione e degli obiettivi di qualità per la protezione della popolazione dalle esposizioni ai campi elettrici e magnetici alla frequenza di rete (50 Hz) generati dagli elettrodotti," *Gazzetta Ufficiale*, No. 200, Aug. 29th, 2003 (in Italian).

7. Buchholz, H., "Elektrische Stromungsfelder mit Schraubenstruktur," *Elektrische Nachrichten-technik*, Band 14, Heft 8, 264–280, 1937.

8. Moser, J. R., R. F. Spencer, Jr., "Predicting the magnetic fields from a twisted-pair cable," *IEEE Trans. on Electromagnetic Compatibility*, Vol. 10, No. 3, 324–329, Sep. 1968.

9. Shenfeld, S., "Magnetic fields of twisted-wire pairs," *IEEE Trans. on Electromagnetic Compatibility*, Vol. 11, No. 4, 164–169, Nov. 1969.

10. Haber, F., "The magnetic field in the vicinity of parallel and twisted three-wire cable carrying balanced three-phased current," *IEEE Trans. on Electromagnetic Compatibility*, Vol. 16, No. 2, May 1974.

11. Hagel, R., L. Gong, and R. Unbehauen, "On the magnetic field of an infinitely long helical line current," *IEEE Trans. on Magnetics*, Vol. 30, No. 1, 80–84, Jan. 1994.

12. Ehrich, M., J. Kuhlmann, and D. Netzler, "Models of a cable bunch formed by twisted three-phase cables," *Proceedings EMC'97*, 463–466, Beijing, China, May 1997.

13. Pettersson, P. and N. Schönborg, "Predicting the magnetic field from twisted three-phase arrangement," *IEEE International Symposium on Electromagnetic Compatibility*, 513–517, Austin, USA, Aug. 18–22, 1997.

14. Mazzanti, G., M. Landini, and E. Kandia, "A Simple Innovative Method to Calculate the Magnetic Field Generated by twisted three-phase power cables," *IEEE Transactions on Power Delivery*, Vol. 25, No. 4, 2646–2654, Oct. 2010.

15. Mazzanti, G., M. Landini, E. Kandia, C. Biserni, and M. Marzinotto, "Innovative calculation methods of the magnetic field from single and double-circuit twisted three-phase cables widely used in MV and LV installations," *Central European Journal of Engineering, Versita Publ. (co-publ. Springer-Verlag)*, Vol. 2, No. 2, 212–223, Jun. 2012.

16. Karady, G. G., K. E. Holbert, S. G. Adhikari, and M. L. Dyer, "Survey of underground cable generated magnetic fields in a residential subdivision," *Proceedings of the Transmission and Distribution Conference and Exposition 2008 (T&D. IEEE/PES)*, 21–24, Chicago, IL, USA, Apr. 2008.

17. Holbert, K. E., G. G. Karady, S. G. Adhikari, and M. L. Dyer, "Magnetic fields produced by underground residential distribution system," *IEEE Trans. on Power Delivery*, Vol. 24, No. 3, 1616–1622, Jul. 2009.

18. Standard CEI-UNEL 35011, Cavi per energia e segnalamento, Sigle di Designazione, 2nd Edition, 2000 (in Italian).